

OBSERVATIONS OF ATMOSPHERIC OZONE ABOVE BANGALORE (13°N LATITUDE) AT 110.836 GHz

M. VIVEKANAND and R. S. ARORA

Raman Research Institute, Bangalore 560 080, India.

ABSTRACT

In the course of radioastronomical observations at Bangalore (13°N latitude), of emission spectra in the mm-wave region of the electromagnetic spectrum, the strong emission line at 110.836 GHz from atmospheric ozone was observed. The present paper shows how using this essentially simple ground-based technique, and a radiative transfer model, continuous cost-effective measurements of the height-distribution of ozone can be made.

1. INTRODUCTION

ATMOSPHERIC ozone has been regularly monitored on a global basis by a network of Dobson ozone spectrophotometers^{1,2} and more recently by means of solar ultraviolet backscatter recording instruments (BUV) and total ozone mapping spectrometers (TOMS) carried on satellites³. *In situ* measurements of ozone have also been carried out for many years by balloon and rocket-borne ozonesondes. Most of these methods require the sun as the source of radiation, based as they are on the absorption by ozone of solar radiation in the ultraviolet and infrared regions of the solar spectrum. Very recently a new technique of ozone measurement has been developed which involves the observation of spectral lines emitted by ozone in the mm-wave region of the electromagnetic spectrum⁴⁻⁶. Since this is an emission measurement, ozone can be observed during both day and night. Calibration methods are also well established at mm-wavelengths⁷. In this paper we report the measurement of ozone in one of its strong spectral lines at 110.836 GHz, using a mm-wave receiver which was constructed for use in radioastronomical studies.

Ozone, an 'asymmetric top' molecule, has a number of rotational transitions which lie in the mm-wave region. For radio astronomers, the $6_{0,6} \rightarrow 6_{1,5}$ rotational transition at 110.836 GHz is particularly convenient, since it lies close to the $J_{1 \rightarrow 0}$ transition of the CO molecule (115.271 GHz), which is extensively distributed in the interstellar medium, and is widely studied by astronomers. Section 2 of this paper gives a brief description of the receiver for CO observations built at the Raman Research Institute. It also describes the spectrometer and the computer-controlled data acquisition system. Section 3 describes the observational

method and § 4 the analysis procedure. We conclude the paper with our preliminary results and a discussion.

2. EQUIPMENT

The first part of the receiver known as the 'front end' is a heterodyne system which down-converts the radio frequency signal at 110.836 GHz (RF) to an intermediate frequency of 1.4 GHz (IF), by mixing it with a locally generated signal of 112.236 GHz (LO). The LO is derived from a water cooled klystron which gives an output power of ~10 milliwatts, which is sufficient to drive the mixer. In order to obtain the required frequency stability, the klystron is phase-locked to a highly stable reference signal derived from a frequency synthesizer. The RF, which is picked up by the feed horn, and the LO which is available as the klystron output, are coupled by means of a 'directional filter' into the mixer. In addition to coupling the two signals, the directional filter also suppresses the LO sideband noise at 1.4 GHz, which would otherwise degrade the receiver noise temperature. The mixer consists of a Schottky-barrier diode operating at room temperature and placed in a reduced height waveguide. The 1.4 GHz IF is amplified by a low noise GaAs FET amplifier, and further down-converted to a final IF of 150 MHz, which is then fed to the 'back end' spectrometer. By using Eccosorb loads, at room temperature and liquid nitrogen temperature, placed in front of the feed horn, we measured the single-sideband receiver noise temperature to be 1500° K. The receiver frequency could be adjusted anywhere between 110 GHz and 120 GHz by mechanically tuning the klystron.

The back end spectrometer consists of a filterbank, which has 256 channels each of half width

250 kHz. It covers a total range of 64 MHz, centred at the final IF of 150 MHz. By a scheme of further IF processing, the 64 MHz input band is broken up into eight bands of width 8 MHz each. Each of these bands is separately amplified and fed into the corresponding part of the filter-bank, each of which contains 32 channels. The output of each filter is square-law detected. In this manner 256 analogue d.c. outputs are available from the filter-bank, each of which is proportional to the corresponding input power to that filter.

The filter-bank outputs are connected to a data acquisition system (DAQ) which interfaces with an LSI-11 computer. For every msec, the DAQ samples each of the 256 analogue inputs, digitizes them by means of an 8 bit analogue-to-digital converter and integrates the data into an internal buffer, for a time specified by the user. It then latches the integrated data into an output buffer, and signals to the computer the end of the integration. The internal buffers are then cleared and integration of fresh data continues. Before the end of the current integration, the computer transfers the latched data into its internal memory. Thus ozone can, in principle, be observed continuously for many hours at a stretch and observations over many days can be added up in the computer.

3. OBSERVATION PROCEDURE

Three observations of ozone emission were made in January and February 1985. The receiver horn was fed at the Cassegrain focus of a 15 cm parabolic dish antenna which gave an effective beam width of one degree. The receiver box with the 15 cm antenna mounted on it was positioned such that it pointed at a zenith angle of $\sim 70^\circ$. To reduce the effects of receiver gain variations, the frequency-switched mode of observation was adopted. This gave the ON-frequency data when the receiver was tuned to the centre of the ozone line, as well as the OFF-frequency data when the receiver was tuned to a band 64 MHz away. The frequency was switched once every 50 msec and the ON and OFF data were separately integrated in the computer. Since no real detector would have a perfect square-law characteristic and any departure from perfect square-law would introduce nonlinear effects in the outputs, we frequently calibrated all our 256 detector current-voltage curves and used the data to correct the observed detector outputs. Receiver gains were eliminated by forming the quantity (ON-OFF)/OFF which was then normalized by the system tempera-

ture. Due to the frequency response of the front-end, a second order baseline had to be removed from the above data. For this, the central 32 MHz band was omitted (where the bulk of the ozone line is expected) and the adjoining pair of 16 MHz bands was used for baseline fitting. In practice, as the wings of the ozone line extend even beyond 100 MHz from the line centre, our baseline fit procedure would introduce an extra curvature into the observed ozone profile. To correct for this, the same analysis was also carried out on the theoretically computed ozone profile and only then were the two profiles compared. The receiver sensitivity was such that in one minute of integration, we could achieve a signal-to-noise ratio of ~ 5 at the ozone line centre.

Every observation was accompanied by a measurement of the atmospheric optical depth τ_a . This was done by measuring the atmospheric emission at three zenith angles. The observed ozone profile was then scaled up by $\exp(+\tau_a)$ to correct for atmospheric absorption.

4. MODEL FITTING

Details of the model used to compute (theoretically) the observed ozone profile are given by Penfield *et al*⁸ and Shimabukuro *et al*⁵. We have essentially followed their basic procedure.

We assume that ozone exists from the surface of the earth to a height of ~ 100 km. The density distribution of ozone $\rho(h)$ as a function of height h is the quantity of interest in this work and we adopt the following formula after Shimabukuro *et al*⁵:

$$\rho(h) = \frac{4D_0 \exp(h - h_0)/r_0}{[1 + \exp(h - h_0)/r_0]^2} \text{ cm}^{-3}, \quad (1)$$

where D_0 , h_0 and r_0 are respectively the density, height and scale factor of the ozone maximum.

To solve the equation of radiative transfer, we need the temperature and pressure of the atmosphere as a function of height. For our computation we used the values of the International Standard Atmosphere at 15°N latitude⁹ which should be appropriate in a mean sense to the atmospheric conditions above Bangalore (13°N latitude). Since these data are available to a height of 90 km only, we begin our computation from this height.

With these inputs we solve the equation of radiative transfer. The kinetic temperature of ozone lies in the range 200° K to 300° K and $(h\nu/k) \sim 5$ for the ozone line centre. Thus, in this Rayleigh-Jeans

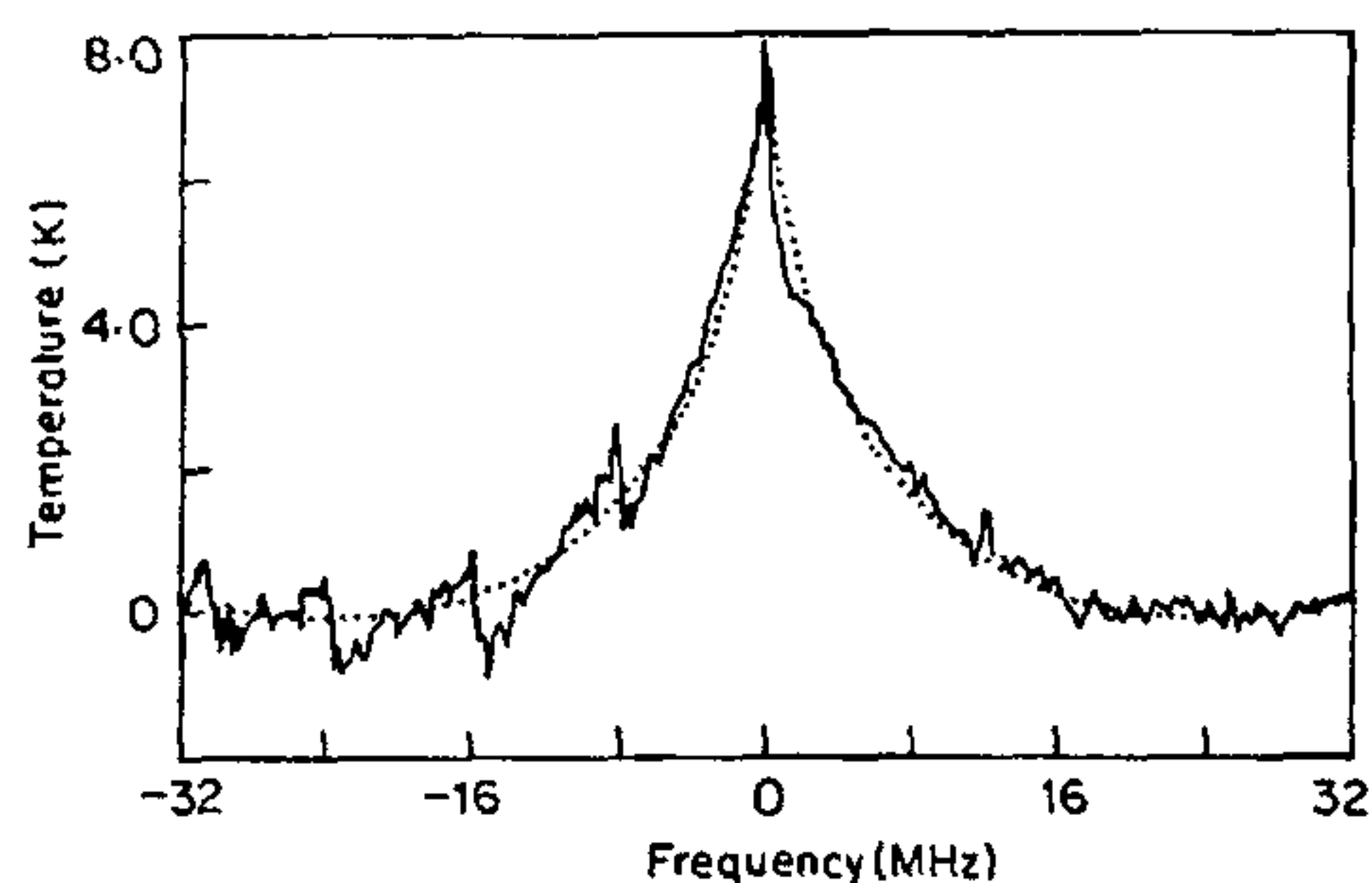


Figure 1. Ozone line observed on 31 January 1985 at midnight, for an integrated time of 120 min. The smooth curve is the theoretical best fit. The line centre lies at 110.836 GHz. A second order baseline was fit to the first and the last 16 MHz data, which was subtracted from the entire profile. The discontinuities at intervals of 8 MHz in the observed profile are due to non-linearities in the back-end spectrometer.

limit, the equation of radiative transfer reduces to

$$dT_0/d\tau(s) = -T_0 + T_a, \quad (2)$$

where T_0 is the brightness temperature of ozone which is the final observed quantity and T_a is the atmospheric temperature. $\tau(s)$ is the optical depth of ozone defined by

$$\tau(s) = \int_0^s k(\nu, s) ds, \quad (3)$$

where the distance s begins at a height 90 km and increases with a decrease in height. $k(\nu, s)$ is the absorption coefficient of ozone, whose frequency

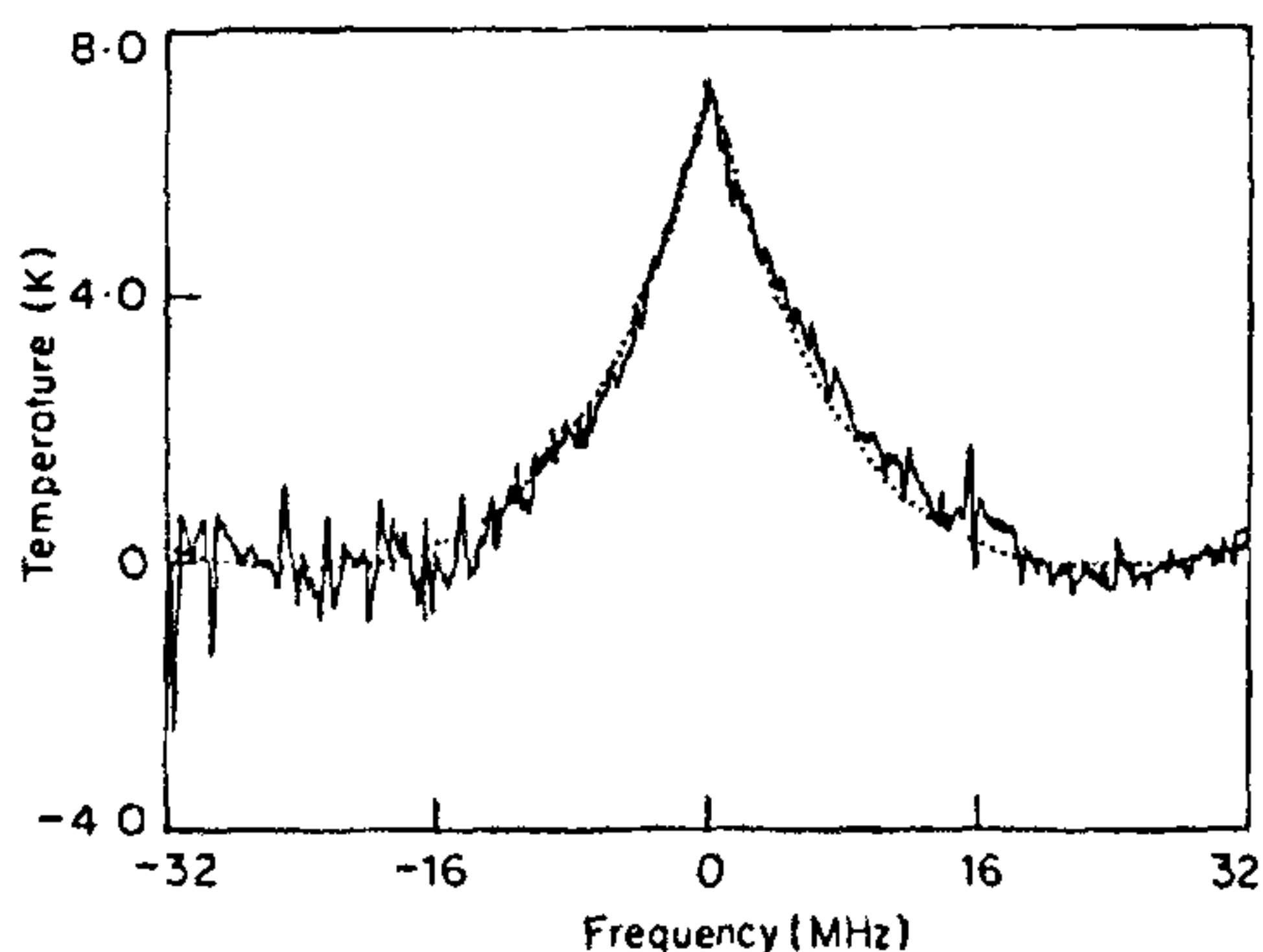


Figure 2. Ozone line observed on 24 February 1985 at 1600h local time, for an integrated time of 60 min.

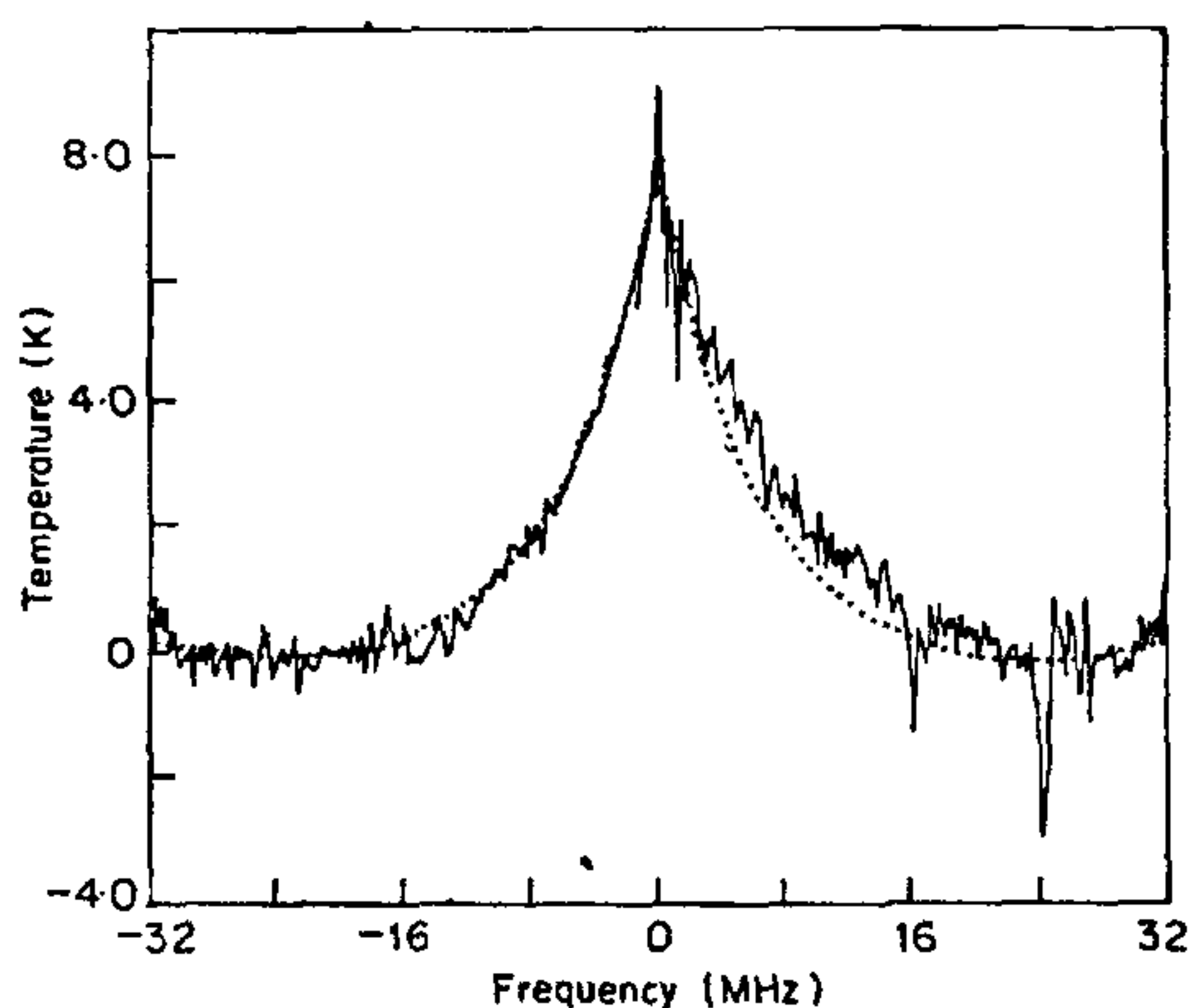


Figure 3. Ozone line observed on 25 February 1985 at 2100h local time, for an integrated time of 60 min.

dependence is determined by both the temperature and pressure¹⁰.

$$k(\nu, s) = \frac{1.7 \times 10^{-24} \rho(s) \nu^2 \phi(\nu, s) \exp[-25.3/T(s)]}{T(s)^{5/2}} \text{ km}^{-1}, \quad (4)$$

where $\rho(s)$ and $T(s)$ are the density and kinetic temperature of ozone as a function of height, ν is the frequency and $\phi(\nu, s)$ is the line profile of ozone at various heights. We obtain $\phi(\nu, s)$ by computing the pressure and temperature broadening of ozone at all heights using the following scheme. At heights above 88 km we use the Doppler broadening Gaussian profile. At heights below 57 km we use the pressure broadening Lorentzian profile. At the intermediate heights we use the Voigt profile which is a convolution of the above two.

We begin the numerical integration of (2) at height 90 km where $s = 0$ and continue till s reaches 90 km at the surface of the earth. At each height the frequency distribution of the ozone line is computed

Table 1 Best fit values of the three parameters of (1) for the three observations carried out in 1985. The statistical errors due to the fitting procedure are $\sim 50\%$ in D_0 and $\sim 10\%$ in r_0 and h_0

	31 January	24 February	25 February
D_0 (cm^{-3})	6×10^{12}	6×10^{12}	5×10^{12}
r_0 (km)	5	3.5	4
h_0 (km)	30	35	35

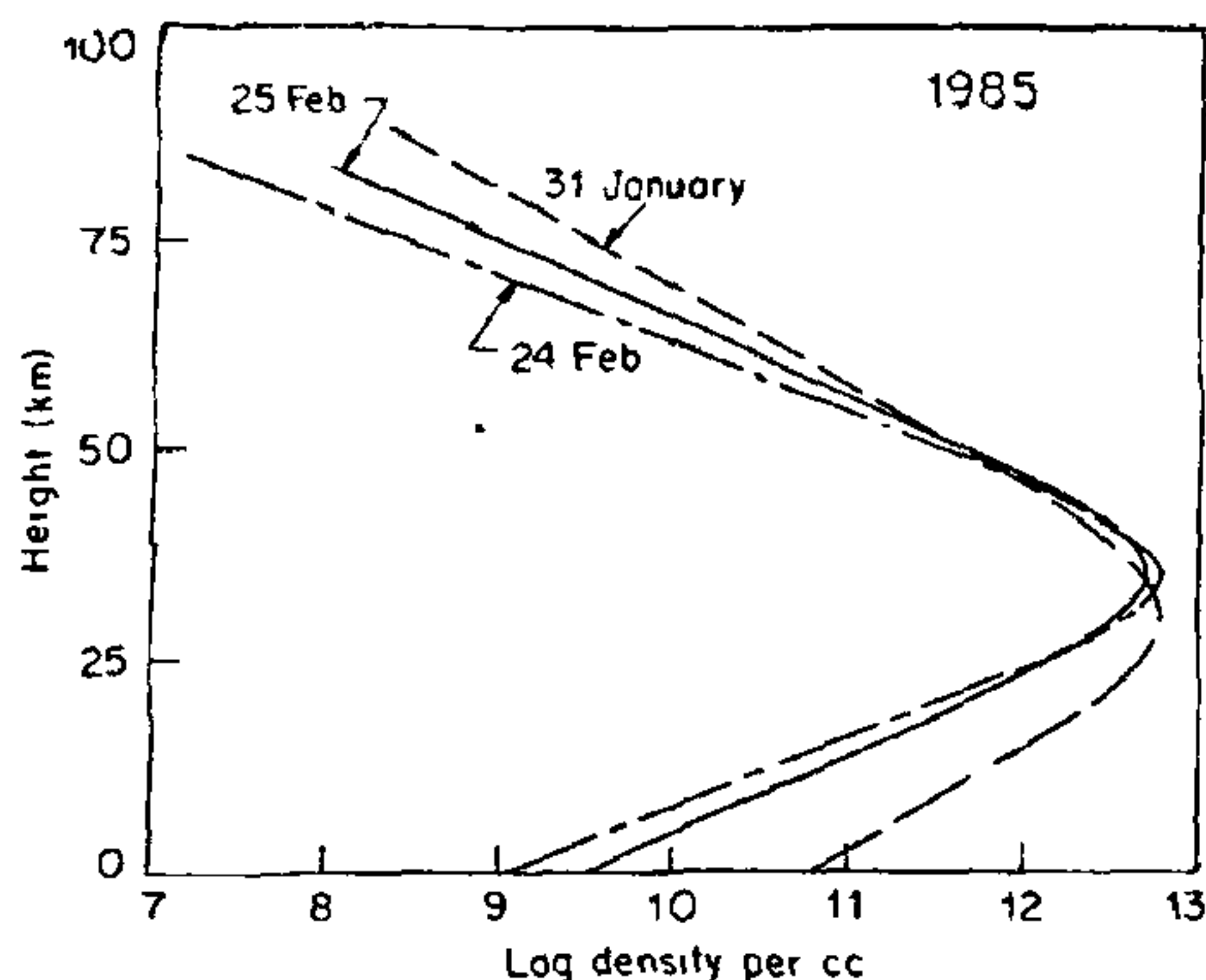


Figure 4. The number density of ozone molecules as a function of height above earth, as given by equation (1).

and the equivalent contribution in 256 frequency channels, each of width 250 kHz, is estimated. At the end of the integration we are left with 256 brightness temperatures corresponding to our 256 frequency channels. These numbers can then be compared with our observations.

5. RESULTS AND DISCUSSION

Figures 1–3 present our observations on 31 January 1985 at midnight (120 min of integration), 24 February 1985 at 1600h local time (60 min of integration) and 25 February at 2100h (60 min of integration) respectively. In each figure the smooth curve is the best fit to the data by the above mentioned procedure. The systematic deviations of the theoretically computed ozone profile from the observed data are due to the nonlinearities in the back-end spectrometer. We are currently in the process of installing a new 150MHz wide acousto-optic spectrometer which should eliminate these instrumental effects.

Table 1 lists the best fit values of D_0 , h_0 and r_0 obtained for each of the observations. These are consistent with the values obtained by De La Noe

*et al*⁶, though we appear to obtain a higher h_0 . The height distribution of ozone density obtained from (1) for the three observations is plotted in figure 4.

These observations, carried out for the first time in India, show that the ground-based mm-wave technique can be effectively and inexpensively used to make routine measurements of the height-distribution of atmospheric ozone. Co-ordinated measurements over a length of time should enable one to arrive at the accuracy of this measurement-technique compared to the other techniques (e.g., Umkehr) now in extensive use.

ACKNOWLEDGEMENTS

The authors thank N. V. G. Sarma and P. Dierich for encouragement and Anna Mani for useful discussions.

5 October 1988

1. Ramanathan, K. R. and Kulkarni, R. N., *Q. J. R. Meteorol. Soc.*, 1960, **86**, 144.
2. Khrgian, A. Kh., *The physics of atmospheric ozone*, 1973, Gidrometeoizdat, Leningrad.
3. Bowman, K. P. and Krueger, A. J., *J. Geophys. Res.*, 1985, **90**, 7967.
4. Schanda, E., Fulde, J. and Kunzi, K., *Astrophys. Space Sci. Lib.*, 1976, **61**, 135.
5. Shimabukuro, F. I., Smith, P. L. and Wilson, W. J., *J. Appl. Meteorol.*, 1977, **16**, 929.
6. De La Noe, J., Baudry, A., Perault, M., Dierich, P., Mannanteuil, N. and Colmont, J. M., *Planet. Space Sci.*, 1983, **31**, 737.
7. Penzias, A. A. and Burrus, C. A., *Annu. Rev. Astron. Astrophys.*, 1973, **11**, 51.
8. Penfield, H., Litvak, M. M., Gottlieb, C. A. and Lilley, A. E., *J. Geophys. Res.*, 1976, **81**, 6115.
9. Shea, L. (ed.), *Handbook of geophysics and space environments*, Office of Aerospace Research, 1965, p. 2, USA.
10. Shimabukuro, F. I., Smith, P. L. and Wilson, W. J., *J. Geophys. Res.*, 1975, **80**, 2957.